Spatiotemporal variability in groundwater chemistry of a mountainous catchment with complex geologic and climate gradients in south west India

J A Gayathri
NCESS: National Centre for Earth Science Studies
Vipin T Raj
NCESS: National Centre for Earth Science Studies
K Sreelash
NCESS: National Centre for Earth Science Studies
K Maya
NCESS: National Centre for Earth Science Studies
M Vandana
NCESS: National Centre for Earth Science Studies
D Padmalal (drdpadmalal@gmail.com)
NCESS: National Centre for Earth Science Studies

Research Article

Keywords: Hydrogeochemistry, Chemical weathering, rock-water interaction, Western Ghats, Southwest India

Posted Date: March 10th, 2021

DOI: https://doi.org/10.21203/rs.3.rs-212826/v1

Version of Record: A version of this preprint was published at Environmental Earth Sciences on August 16th, 2021. See the published version at https://doi.org/10.1007/s12665-021-09862-6.

Abstract

Mountainous catchments are one of the world's important water sources that sustains a major portion of global population and a rich biodiversity. The groundwater quantity and quality of mountainous watersheds are depended generally on the geologic characteristics and climate gradients. Although many groundwater studies have been carried out in the midlands and lowlands of many river basins, not enough focus has been paid to the mountainous catchments of tropics. Here we report a case study on groundwater quality and controlling factors of a mountainous catchments of the Western Ghats mountain ranges of peninsular India - the Bhavani river basin, which is identified as a testbed for long-term monitoring of the Critical Zone process. A total of 88 water samples were collected seasonally for assessing various physico-chemical parameters, solute contents and scaling properties. The results of the study revealed that the hydrochemistry of groundwater is influenced by both silicate and carbonate weathering. Mineral stability indices computed for the groundwater reveal that about 52 % of the samples are supersaturated with carbonate minerals and often exhibit scaling due to solute overloading. Among the contributing factors that determine water quality of groundwaters, chemical weathering and anthropogenic activities play a significant role.

1.0 Introduction

Mountainous watersheds are considered generally as the world's major water sources that support a significant portion (~ 25%) of global population (Meyback et al., 2001). Although the groundwater contribution to mountainous stream flow was once assumed to be relatively small, it is now regarded as an important water source to streams and the people residing in the area and/or further downstream. Over-dependence on the groundwater resources and human interventions in the catchments has often led to large-scale decline in the quantity and quality of the groundwater resources even in mountainous catchments (Guo and Wang, 2005; Peisert and Sternfeld, 2005; Vaux, 2007; Sadoff and Muller, 2009; Padmalal et al.,2011; Vaux, 2011; Hallouche et al., 2017; Kaushal et al.,2017). Social and economic activities of the catchments are mostly dependent on the availability and quality of groundwater for various purposes (Hosseinifard and Aminiyan, 2015; Elgallal et al., 2016; Chandran et al., 2017; Wu et al., 2017; Jampani et al., 2018 and Pincetti-Zúniga et al.,2020). Among the water quality related problems, scaling and solute overloading are one of the major concerns in mountainous catchments with complex geo-environmental settings. As per the United Nations Sustainable Developmental Goal-6 (SDG-6), ensuring the availability of potable water resources for human uses and other economic developments is of prime importance to every nation. A comprehensive understanding of the hydrogeological systems - their behaviour, interaction and evolution etc., is more pressing than ever (Sophocleous, 2010).

Groundwater chemistry is dependent on several factors including the nature of recharge, the residence time of groundwater in the aquifer, rock-water interaction beneath the surface, chemical weathering rates and anthropogenic activities (Andre *et al*., 2005; Ekwere and Edet, 2012; Loh et al., 2016; Rao et al., 2019 and Sivakarun N, et al., 2020). Each groundwater system in an area has a distinctive suite of chemical components, which is attributed as a result of chemical changes in the rainwater as it percolates through

the aquifer system (Back,1966; Derver,1988; Zhu et al., 2004). Analysis of hydrochemical data of the aquifers could provide useful information on the geo-chemical evolution of the groundwaters (Gerla,1992). Therefore, it is essential to determine the processes that control groundwater chemistry for effective water resource management and conservation (Jeong, 2001; Edmunds et al., 2002). In most cases, specific molar ion ratios are useful in evaluating the sources of solutes and characterizing their hydrogeochemical make up (Barzegar, 2017; Voutsis, et al., 2015). Various factors such as precipitation, dissolution, oxidation-reduction reaction, chemical weathering of different rock types, evaporation, and ion exchange reactions play a significant role in contributing ionic constituents to the groundwater (Moran-Ramirez *et al*., 2016). Apart from these geogenic processes, anthropogenic factors also play a pivotal role in determining the quality of groundwater in human stressed areas. Here we report a case study from the mountainous catchments in the Southern Western Ghats which is least addressed although the groundwater quality exhibits marked spatial heterogeneity and often leading to even solute overloading and scaling. Considering the unique characteristics of the mountainous catchments of the Bhavani river, the region is now chosen as a test bed for critical zone studies by the National Centre for Earth Science Studies (NCESS) under the Ministry of Earth Sciences (MoES), Government of India.

2.0 Study Area And Its Geo-environmental Setting.

The area upstream of the Pillur reservoir in the Bhavani river has been considered for the present study as the area forms the master watershed chosen for CZO- based investigations (Fig. 1). The area spreads between E longitudes 76° 26’0” – 76° 50’0” and N latitudes 10° 54’0” – 11° 26’0” with a total coverage of 1223 km^2. The basin comprises an undulating terrain with elevations vary between 360 m and 2618 m above sea level. Bhavani river is the second largest tributary of the Cauvery river, which originates from the southwestern flanks of the Nilgiri hills of Western Ghats mountain ranges. The river enters Kerala through the Silent Valley reserve forests in the Palakkad district. It drains through the Attappadi valley, and takes a ninety degree turn at Mukkali and thereafter flows northeasterly before merging with the master channel of the east flowing Cauvery river. Geologically, the watershed forms a part of the highly deformed polymetamorphic Pre- Cambrian terrain of peninsular India. The study area comprises of a spectrum of rock types including charnockite, hornblende gneiss, quartz-biotite schist, quartzite, biotite granite gneiss, granite and layered igneous complexes with basic and ultra-basic rock formations (Fig. 2). The oldest rock unit in Attappadi could be equated with Archean Sagur Group of Karnataka and Wayanad Group in Kerala. The Wayanad group at Attappadi includes conglomerate, metapelites, fuchsite quartzite, ultramafics, amphibolites, anorthosite, talc-tremoliteschist, felsic rocks and banded iron formation (Nambiar, 1982, Nair et al, 2005). Sulfide-rich rock formations are also reported from certain locations of the study area. The charnockite rock formations are confined mainly to the north of the Bhavani River basin. Biotite gneiss, hornblende gneiss and younger migmatite complexes constitute the Bhavani Group (Nair et al, 2005; Santosh et al, 2013). Granite emplacements have been observed in the southeastern part of the study area. Laterite cap rocks are present in the southwestern part. Occurrence of kankar (a form of $CaCO_3$) nodules is widespread in the soil profile at the eastern part of the study area (Mining and Geology, 2016). The area exhibits a variety of land use categories which include agricultural land, built-up areas,

forest, grassland, grazing land, and water bodies. Geomorphologically, the Bhavani river basin considered for the present study can be divided into six major units such as denudational hills, valley fills, pediments, lateritic uplands, and rivers; among which the denudational hills dominate the topography. The denudational hills and pediments can be further divided into sub-units such as denudational hill-high, medium and low, buried pediments.

The study area hosts two distinct climatic zones; the southern and the western parts receive maximum rainfall during the southwest monsoon (June to September) while the eastern part receives rainfall mainly from the northeast monsoon (October to December). The western portion is generally wet, warm, and humid for almost nine months in a year, whereas the eastern part remains almost dry and warm throughout the year. The Silent Valley National Park located in the upper part of the basin receives an annual rainfall of more than 4000 mm, while the eastern half of the study area receives precipitation of 1500 mm only. The area, in general, enjoys a very hot climate during summer and pleasant climate in the winter season. The average day temperature during winter is about 30˚C and in summer, the maximum day temperature is about 40˚C.

3.0 Materials And Methods

Groundwater samples from 23 open wells and 21 bore wells were collected from the study area during pre-monsoon and post monsoon seasons and were analyzed for various physico-chemical parameters. The sampling locations are depicted in Fig. 2. The depth of the open wells ranges from 3 to 18 m and bore wells from 90 to 182 m. The water samples were collected in well cleaned polyethylene bottles after thorough rinsing with the water to be sampled.

The pH, EC, Dissolved Oxygen (DO) and Temperature of the water samples were estimated in the field using a portable water quality analyzer (EUTEC650). Water samples were filtered using a 0.45µm membrane filters to separate out suspended particles and then used for the hydrochemical analysis following standard procedure (APHA, 2005). Major cations like Ca and Mg were analyzed titrimetrically using EDTA, while Microwave Plasma Atomic Emission Spectroscopy (Agilent 4210 MP-AES) was used for the estimation Na^+ and K^+. Carbonate (CO_3^{2-}) and bicarbonate (HCO_3^-) ions were measured volumetrically using 0.2N H_2SO_4 and Chloride (Cl^-) by argentometric method (APHA,1995). Sulfate ($SO4^{2-}$) was measured by the $BaCl_2$ method using a UV spectrophotometer (Shimadzu UV-160A), and silicate was determined using Continuous Flow Analyzer (Model: SAN++). Normalized inorganic charge balance was applied to evaluate the accuracy of results, and the ionic charge balance error was found to be less than 10%. Piper diagram (Piper 1953) was drawn using Aquachem software to classify the major water types to interpret the hydrochemistry of the area. Durov diagram is plotted using the Geochemist's Workbench v.4 and the diagram is plotted based on the milliequivalent percentage of the total major cations and the total major anions in the water samples. Spatial variation maps of TDS, major cations, and anions were produced using the inverse distance weighted (IDW) interpolation method of ArcGIS 10.3. The spatial pattern of parameters was analyzed in two seasons, i.e., pre-monsoon, post-monsoon

seasons for both open well, and bore well samples. The geochemical software PHREEQC v2.16, and Geochemist's Workbench v.4.was used to calculate saturation indices and log activity values of waters. Saturation indices (S.I.) were calculated as the log of the ratio between the ion activity product and the equilibrium constant. Bivariate diagrams of Ca + Mg vs HCO_3, Ca + Mg vs HCO_3 + SO_4, Na vs Cl, Na + K vs Cl + SO_4, Na + K vs total cations and Ca + Mg vs total cations, mineral stability diagrams were plotted to understand the hydrochemical processes and to reveal the stable mineral phases existing in the study area. Scaling properties of water samples were determined by using the Langelier saturation index (LSI) (Langelier, 1936) and Puckorius scaling index (PSI) (Tyagi and Sarma, 2020).

The multivariate statistical method has been used to study relationships existing among the samples and to obtain vital information from hydrochemical data sets using the statistical software package SPSS version 16. Pearson correlation analysis, Principal component analysis, (PCA) Agglomerative Hierarchical cluster analysis (AHC) was performed to classify groundwater samples and to identify the relation existing among the chemical parameters and groundwater samples. Principal components are obtained by multiplying the eigenvector (loadings) with the original correlated variables. Eigen values of the principal components are the measure of their interrelated variance. Principal components are extracted in a way that the greatest variance of the observed data is accounted by the first component, the second greatest variance by the second component, and so on. (Selle et.al 2013). Principal components with an eigen value greater than one is considered to account for the maximum variance in the observed parameter (Kolsi et al. 2013). Varimax rotations are applied to all the extracted principal components to reduce the contribution of the variables that are not significant (Closs and Nichol, 1975). Each variable considered for PCA has a weight factor associated with it. This weight factor, also referred to as the PC score, is the correlation between the original variable and a factor. A PC score close to ± 1 indicates a strong correlation between the given variable and factor. After the interpretation of each factor, the contribution of each factor scores at each well was computed, analyzed the effect of each factor on samples and quantified similarity of samples. Agglomerative hierarchical cluster analysis (HCA) was used to classify the samples into discrete hydro chemical groups based on their similarity. Ward linkage method and Squared Euclidean distance are applied in the analysis to produce the most distinctive groups. AHC classifies the data in a relatively easy and direct manner, with the results being presented as a dendrogram.

4.0 Results And Discussion

4.1 *Well water chemistry – Open wells and bore wells*

The physico- chemical parameters estimated for the groundwater samples of the study area are given in Tables 1 and 2. Fig. 3 (a & b) depicts the hexa plots worked out for the open and bore well waters with respect to the sampling stations. The pH of the open well samples vary from 6.1 to 7.87 and 6.1 to 7.57 during pre-monsoon and post-monsoon seasons, respectively. Higher pH values are observed for the wells dug out in the talc-tremolite dominated areas where pH of water was slightly alkaline (7.45 to 7.87). At the same time, lower pH values were observed in the charnockite dominated areas. Spatial analysis

reveals that slightly acidic pH in open well waters were noticed in the western part of the study area dominated by charnokites. Further, the region experiences high rainfall and humid climate. The electrical conductivity (EC) values for open well samples during pre-monsoon and post-monsoon seasons ranged from 154 to 1260 µs/cm and 77 to 1046 µs/cm, with averages of 705 µs/cm and 540 µs/cm, respectively. Like the case of pH, high EC values (792 to 1260 µs/cm) were observed in the talc- tremolite dominated areas. At the same time, low EC values were noticed in charnockitic terrains, irrespective of seasons. TDS values show wide variation in both pre-monsoon (100 to 830 mg/l) and post-monsoon (50-680 mg/l) seasons. The content of calcium during pre-monsoon and post-monsoon seasons ranges from 7.22 mg/l to 92.2 mg/l (avg. 52 mg/l) and 4 mg/l to 120 mg/l (avg. 56 mg/l) respectively. The concentration of calcium values shows an increasing trend from the western part to the central part of the basin. Magnesium also shows a trend similar to that of calcium but the values are slightly lower [pre-monsoon: 6 mg/l to 56.7 mg/l (avg.23); post-monsoon 2.4 mg/l to 31 mg/l (avg.12)]. The seasonal average of sodium concentration of open well samples was 25.8 mg/l (3.8 mg/l to 45.7 mg/l) and 12.64 mg/l (1.6 mg/l to 35.1 mg/l) during pre-monsoon and post-monsoon season, respectively. High sodium values were observed in the moist, sub-humid climatic zones occupied by talc- tremolite and charnockite rocks. The values of potassium were generally low compared to the other major cations. The average concentration of potassium was 3.9 mg/l (1.1 mg/l to 12.6 mg/l) during the pre-monsoon season and 3.3 mg/l (0.37 mg/l to 10.3 mg/l) during the post-monsoon season. Bicarbonates, chlorides and sulfate constitute the major anions in the open well water samples. The averages and ranges of bicarbonate were 268 mg/l and 50 - 540 mg/l in pre-monsoon season and 194 mg/l and 25- 420 mg/l during post-monsoon season. The higher concentration of HCO_3^- was noticed for the sample OW21 during both pre-monsoon and post-monsoon seasons. Chloride ranges from 7 mg/1 to74 mg/1 and 5 mg/1 to 52 mg /1 with an average of 39 mg /l and 30 mg/1 during pre-monsoon and post-monsoon seasons. Higher chloride values were observed in the regions close to agricultural lands and settlements. The seasonal average of SO_4^{2-} concentration of the open well sample was 21 mg/l and 15 mg/l during pre-monsoon and post-monsoon seasons, respectively. Samples in the talc-tremolite and granite gneiss dominated areas show considerably high sulfate values (24 mg/l) compared to areas dominated by other rock types (12 mg/l). The order of dominance of the cations in the open well water is $Ca^{2+} > Mg^{2+} > Na^+ > K^+$ in (mg/l) and that of the anions is $HCO_3^- > Cl^- > SO_4^{2-}$.

In the case of the bore well waters, variation of pH during pre-monsoon and post-monsoon seasons were 6.9 to 7.94 (avg.7.43) and 6.5 to 7.9 (avg.7.4) respectively, which are almost similar to that of the open wells. Higher pH values were observed in talc- tremolite rock dominated areas and low in the biotite gneiss dominated areas. On an average, the EC values of the bore well samples are quite higher during pre-monsoon (1132 mg/l) and post-monsoon seasons (824 mg/l). Higher EC values (i.e., greater than 1800 µs/cm) were observed in two bore well samples BW10 and BW12 – drilled in quite complex lithology. Samples collected from the talc- tremolite schist dominated areas show high EC values. The TDS values range from 230 to 1515 mg/l (avg.750mg/l) and 138 to 1037 mg/l (avg.539 mg/l) during pre-monsoon and post-monsoon seasons, respectively. The content of Ca during pre-monsoon and post-monsoon seasons were between 22 to 185 mg/l (avg.88 mg/l), and 28 to 168 mg/l (avg. 91 mg/l/). An

increase in the Ca values is noticed in the samples collected from talc-tremolite dominated regions during post-monsoon whereas lower values are noticed in the granite gneiss dominated regions. Magnesium in the bore well waters ranges from 10 to 78 mg/l (avg.38) and 2.4mg /l to 59 mg/l (avg.23) for the pre monsoon and post monsoon seasons. The highest magnesium values were estimated for the sample BW17 which was drilled in the talc- tremolite rock dominated area. Bore well samples in the charnockitic terrains gave lower values. The seasonal average of Na concentration of bore well samples was 41 mg/l and 23.3 mg/l during pre-monsoon and post-monsoon seasons, respectively. The concentration of potassium in the bore well samples ranged from 2.6 mg/l to 14.4 mg/l during the pre-monsoon season and 1.1 mg/l to 9.2 mg/l during the post-monsoon season. Higher concentration of K was observed for the sample BW8 and BW19 and these wells are drilled in the pyroxenite rock dominated area. The seasonal bicarbonate (HCO_3) concentration of bore well samples range from 100 mg/l to 660 mg/l (avg. 400 mg/l) during pre-monsoon and 54 mg/l to 580 mg /l (avg. 298mg/l) during post-monsoon seasons. The ranges of Cl values during pre-monsoon and post-monsoon season were 14.1 – 102 mg/1 (avg. 44 mg /l) and 10 – 96.5 mg /1 (avg. 39 mg /l), respectively. High chloride values were noticed in the wells in the pyroxenite rock dominated areas that are situated close to agricultural lands. The SO_4 concentration of the bore well samples range from 7 mg/l to 508 mg/l (avg. 78 mg/l) and 3.8 mg/l to 285 mg/l (avg. 49 mg/l) during pre-monsoon and post-monsoon seasons. Higher sulfate values were observed in the two samples such as BW10 and BW12 that were drilled in complex suite of rocks. The order of abundance of the cations in the bore well waters, is $Ca^{2+} > Mg^{2+} > Na^{+} > K^{+}$ in (mg/l) and that of anions is $HCO_3^{-} > Cl^{-} > SO_4^{2-}$.

4.2 Spatial variation of groundwater chemistry

Figure 4 shows the distribution of TDS in the open well and bore well samples during pre- monsoon and post-monsoon seasons. In general, the geo- spatial trends in the concentration of the studied parameters are almost same in the case of open wells and bore wells samples; however, marked variation in concentration is noticed between the wells. The average concentration of TDS in the bore well water is markedly higher than open well waters in both the seasons (Fig. 4). Based on the spatial variability of the solute loading, the study area is classified into two zones: 1) Zone having high solute loading noticed in the central part (areas like Palur, Chavadiyur, Agali) 2) Low solute containing waters in southwestern part of the study area (areas like Chemannur, Virannur, etc). The spatial distribution of ions within the Bhavani basin is more significant for TDS, $Ca^{2+,}$ Mg^{2+} Na^{+}, $HCO_3^{-}$and SiO_2^{-}. Major ions show a tendency to be present at higher levels towards the central zone of study area where the climate is sub-humid and the lithology is essentially amphibolites, anorthosites and talc – tremolite schist.

In the case of borewell samples, high TDS zones were identified in the central part of the study area where the values range 1000 mg/l to 1515 mg/l as against the concentration of 750 – 830 mg/l in the open wells. Post-monsoon season also shows the same trend but the values are low compared to the pre-monsoon season and this may be due to dilution by the percolating rain water.

Calcium enrichment zones were identified in the central part of the study area, and values are decreasing gradually towards the southwestern area, both in the case of open well and bore well samples. This part of the area experiences a humid climate and calcium values are low for open well and bore well samples irrespective of the seasons. Calcium enrichment zones in the central part of basin are mainly due to the sub-humid climate and alteration of calcium-rich minerals in the host rocks such as meta-pyroxenites, amphibolites, anorthosite and talc-tremolite schist. Leaching of Kankar, the near-surface accumulations of calcium carbonate, formed due to evaporation of the capillary waters during pre-monsoon, is also responsible for the observed high calcium content in the groundwater during the post-monsoon samples.

The spatial variation map of magnesium ions indicates nearly a similar trend as that of calcium. Magnesium concentration for both open well and bore well samples during pre-monsoon and post-monsoon season shows high value towards the central part of the basin (Palur, Kalkandi and Chavadiyur). Magnesium in the central part of the basin is presumably derived from the alteration of magnesite veins in the talc - tremolite schists and other alkaline earth bearing rocks in the areas mentioned earlier.

In the study area, sodium (Na^+) concentration is low relative to calcium and magnesium and shows a slightly different distribution pattern. Individual pockets of higher sodium concentrations for both open well and bore well is being observed in the northeastern and central part of the study area where granite gneiss and talc - tremolite schist are the dominant rock types. Potassium (K^+) shows a particular pattern of distribution with local peaks of concentration values, more than 10 mg/l for both open well and bore well samples. They are located at sampling points OW15, OW18, BW8 and BW19. Pyroxenites and gabbro are the major rock type in these locations and the major source of potassium in groundwater is by weathering of silicate minerals such as feldspars and biotite. Concentration of potassium in natural waters is generally low because of the high degree of stability of potassium-bearing alumino-silicate minerals. The concentration variation of potassium during post-monsoon season shows the same pattern as that of pre-monsoon season.

Bicarbonate is the dominant anion in the study area and the spatial variation of bicarbonate ions (HCO_3^-) indicates a similarity with calcium and magnesium cations, which indicates that the bicarbonate is derived from the weathering of silicate and carbonate rocks in the study area. Highest bicarbonate values are found in the central part of the basin and maximum bicarbonate values noticed for open well and bore well samples during pre-monsoon are 540 mg/l and 660 mg/l respectively. Like the other ionic constituents chloride enrichment zone is also observed in the central part of the basin and decreases towards the southwestern part for both open well and bore well samples. High concentrations are observed in samples OW21, OW22, BW8 and BW19 and these locations are closer to agricultural land and settlements. The spatial distribution of SO_4^{2-} shows a localized sulfate enrichment zone in the case of open well and bore well samples. Higher concentration of sulfate is noticed in two bore well samples (BW10 and BW12) located in central part of the basin. Sulfate in the study area is derived from the dissolution of accessory minerals like pyrite, chalcopyrite and in the host rocks. From the spatial variation

map of silicate, it is inferred that the slightly higher concentration of silicate is observed in the central part of the study area which shows an almost similar trend of Ca, Mg and Na.

4.3 Piper Diagram and Durov diagrams

The geochemical nature of open well and bore well samples could be easily understood by plotting the cationic and anionic concentrations in Piper trilinear diagram (Piper 1953); (Fig. 5). The groundwater (open well and bore well) samples are dominated by the cation Ca^{2+} with appreciable amount of Mg^{2+} ions. The alkali element content is substantially low in the samples compared to the alkaline earths. In general, the post-monsoon samples are more enriched with Ca than the pre-monsoon samples. In the case of Mg^{2+}, comparatively high values are noticed in the pre-monsoon samples. The content of HCO_3^- ions dominates in the anionic suite - both in open well and bore well samples, with the exception of two bore well samples in pre-monsoon and post-monsoon (BW10 and BW12) seasons, where in the SO_4^{2-} content enriched in appreciable levels over HCO_3^-. A few bore well samples (BW8 and BW 19) exhibit substantially high amount of Cl in pre-monsoon and post-monsoon seasons. The diamond field in the piper diagram is divided into six subzones Ca-HCO_3, Na-Cl, Mixed $CaNaHCO_3$, Mixed CaMgCl, CaCl and $NaHCO_3$. All the open well samples of the study area fall within the $CaHCO_3$ type; however, a slight shift is noticed in the segregation pattern of the sample plots. The pre-monsoon sample shows a marginal affinity toward the mixed $CaNaHCO_3$ facies field, where as the post-monsoon samples inclined toward the CaCl facies field. The spread of the bore well samples exhibits wide variation compared to the open well samples both the case of pre-monsoon and in post-monsoon seasons. Although most of the samples fall within the $CaHCO_3$ type facies field, the samples BW8 and BW19 in the pre-monsoon and post-monsoon seasons fall within the CaCl type facies field. Like the case of open well samples, the post-monsoon sample plots of the bore wells too exhibit a marked shift toward the CaCl type facies field. The same time, the pre-monsoon sample plots are segregated more towards the CaMgCl facies field. The distribution of the sample plots reveals the fact that the water samples have temporary hardness and alkaline earth (Ca^{2+} + Mg^{2+}) exceeds the alkali (Na^++ K^+) and weak acid (HCO_3^-) exceeds strong acid (Cl^- and SO_4^-) in majority of the samples.

The Durov diagram depicts the evolutionary trends and hydro chemical processes in the groundwater system. The cations and the anions are plotted on their respective triangles; where in the cations occupy the left side triangle and anions the right side. The rectangular field in the diagram is divided into nine fields according to the combination of dominant cations and anions. The parameters such as the total dissolved solids (TDS) and the pH are also added to the remaining sides of the main rectangular field of projection (Fig. 6). From the cationic triangle it is evident that the open well and bore samples are enriched in calcium ions during the postmonsson season. As noticed in the Piper diagram, the Mg ions are enriched in the groundwater during pre-monsoon season. With the exception of the two bore well samples BW10 and BW12, the HCO_3 is enriched in the groundwater samples pre and post-monsoons. Majority of the open well and bore well samples during post-monsoon season falls in the $CaHCO_3$ water type except two open well and three bore samples. Three bores well samples (BW10, BW12 and BW19)

during pre-monsoon season have TDS greater than 1200 mg/l and these samples falls closer to field 5 which indicates a mixed water type formed by dissolution process.

4.4 Multivariate Statistical Analysis

Principal Component Analysis (PCA) and Agglomerative Hierarchical Clustering (AHC) was performed on the hydrochemical data of the open-well and borewell samples of the study area in order to identify the dominant factors controlling the hydrochemical behaviour of groundwater in the region. A total of nine parameters such as, TDS, Ca^{2+}, Mg^{2+}, Na^{+}, K^{+}, HCO_3^{-}, Cl^{-}, SO_4^{2-} and SiO_2 were used for PCA and the principal components with Eigen values less than one were not considered in this study. PCA of the open-well samples highlights two factors with eigenvalues higher than 1 that could explain about 75.34% and 82.22% of the variance in the post-monsoon and pre-monsoon respectively (Table 3). PC1 for the open well samples during post-monsoon season accounts for about for 60 % of the data variability and shows strong factor loadings of TDS, Ca^{2+}, Mg^{2+}, HCO_3^{-} and SiO_2 and moderate positive loading on Na^{+}, Cl^{-}, SO_4^{2-}. The major ions Ca^{2+}, Mg^{2+}, HCO_3^{-} and SiO_2 are associated with hydro chemical variables from mineral weathering and water–rock interactions in the aquifer, which indicates that PC1 reflects the lithological effects. Dissolution of carbonate minerals and dissolution of atmospheric and soil CO_2 gas could be a mechanism supplying HCO_3^{-} to the groundwater. The geogenic factors related to dissolution of Ca and Mg rich minerals highlighted in PC1; however, the significant factor loading of Cl in PC1 can be attributed to the anthropogenic activities mostly related to agricultural activities in the study area. PC2 represents 14 % of the total variance for both pre-monsoon and post-monsoon seasons and has significant strong positive loadings on K and SO_4 which indicates that these elements also have a role in determining the groundwater chemistry of the area, where SO_4 are released from the dissolution of sulfate rich minerals in the area. In the case of bore wells samples, three factors were identified with eigen values greater than 1, with a cumulative explained variance of 81.68 and 85.77 respectively for the post-monsoon and pre-monsoon. PC1 represents about 54% and 55% of the data variability and shows strong factor loadings of TDS, Ca^{2+}, Mg^{2+}, HCO_3^{-}, and SO_4^{2-} for pre-monsoon and post-monsoon seasons. PC2 accounts for about 15% and 18% of the data variability for pre-monsoon and post-monsoon season and shows significant strong positive loading on K and Cl and PC3 shows strong positive loading on SiO_2 for both seasons. PC1 and PC2 have the maximum variance and are mainly responsible for controlling geochemistry of bore well samples. From these it can be inferred that the geogenic factors have a great role in determining the groundwater chemistry of the study area.

The distribution of the principal component loading in space (with respect to individual wells) is shown in the scatter plot of PC1 vs PC2 in Fig. 7. This was performed to determine the dominant controls of the hydrochemistry of the groundwater in the study area. Plot of PC1 versus PC2 in Fig. 7 indicates the wells falls in two distinct groups. The first group (marked in black circles) falls in the negative loading of the PC1 and the second group (marked in red circles) falls in the positive loading of PC1. The wells in the first group is characterized by low concentration of ions as compared with that of the second group. The spatial distribution of the two groups and their factor loading is shown in Fig. 7, which indicates that

majority of the wells in first group lies in the humid part of the study area with an average annual rainfall > 2500 mm. However, most of the wells in the second group lies in the sub-humid to semi-arid part of the study area with an annual average rainfall between 1000 to 1750 mm. This indicates that the climate of the region has a strong bearing on the solute loading of the groundwater samples.

Correlation analysis was performed for the factor loadings of the wells with the elevation, slope, rainfall, potential evapotranspiration (PET), actual evapotranspiration (ET) and PET/rainfall ratio (Table 4). The factor loadings of the wells were found to be highly correlated with the climatic factors (rainfall, PET, ET and PET/Rainfall ratio) as compared to the topographic factors (elevation, slope). The highest correlation of PC1 of open well was found to be ET (-0.76), rainfall (-0.74) followed by PET/Rainfall ratio (-0.62). All these correlations were found to be statistically significant at alpha *= 0.05,* indicating the climatic factors play a major role in determining the quality and quantity of solute loading in the open-well waters of the study area. In the case of bore wells, the highest correlation of PC1 was found to be with ET (-0.51) followed by elevation (-0.41), while the highest correlation of PC2 was found to be with the slope of the terrain (-0.44) followed by elevation (-0.41) indicating that terrain characteristics has a significant role in determining the groundwater chemistry in the bore well waters.

To further substantiate the results, Agglomerative Hierarchical Clustering (AHC) was performed to determine the similarity grouping in the behavior of hydrochemical parameters. The pre-monsoon dataset of open well samples provided two distinct groups as shown in Fig. 8a. About 52% of the open well samples fall in the Group-1 and the remaining 48% of the samples fall in Group-2. Overall, the samples of Group-1 have a TDS less than 300 mg/l, since it is having lowest cations and anion concentrations. The wells in Group-2 have a TDS value greater than 500mg /l. Cluster analysis of well samples during post-monsoon season also shows the almost same trend as that of pre-monsoon samples (Fig. 8b). In the case of bore well (Fig. 8c and 8d), two groups with subgroups are identified, with 28 % and 72 % of the bore wells falling in the Group-1 and Group-2 respectively for the pre-monsoon season. This distinction of groups is based on the ionic concentration as in the case of bore wells. These results show that the climate controlled hydrochemical variability is well reflected in the case of open-well samples which are under the direct influence of rainwater percolation and evapotranspiration as compared to bore wells drilled through hard crystalline rocks.

4.5 Chemical weathering processes in the study area.

Chemical weathering is a major process that results in the evolution of major cations and anions in the groundwater aquifers. Incongruent dissolution of the rock-forming minerals such as pyroxenes, amphiboles and plagioclase will result in the formation of various clay minerals such as kaolinite, montmorillonite, and cations such as Ca^{2+}, Mg^{2+}, Na^{+}, and K^{+} which ultimately added to the groundwater.

The nature and extent of the chemical dissolution is well reflected in the bivariate diagrams (Fig 9a-f). According to Stallard and Edmond (1983), if Na/Cl ratio greater than 1 indicates silicate weathering process. In the present study, about 70% of the pre-monsoon and 13% of the post-monsoon samples have

Na/Cl molar ratio greater than 1, indicating that silicate weathering plays a pivotal role in contributing alkali elements especially Na, to the groundwaters. The remaining samples have Na/Cl less than 1 due to dominance of Cl^- reached either due to base exchange processes or anthropogenic inputs. This is substantiated by the increase in Cl^- ions during post-monsoon season. The rise in water table level in the post-monsoon could dissolve more salts from the upper soil layers affected by agricultural activities. The molar Ca/Mg ratio was used for tracing the sources of these elements; the ratio < 1 indicates dolomite dissolution and > 1 shows calcitic contribution (Mayo and Loucks, 1995). If the molar ratio of Ca/Mg is greater than 2 indicates silicate mineral dissolution which is contributing Ca^{2+} and Mg^{2+} to the groundwaters. In the present study, about 76% of open well samples and 68% of borewell samples in pre-monsoon and 30% of post-monsoon samples have a value between 1 and 2 which indicates that both silicate and carbonate weathering occurs in the area. In the Ca+Mg vs HCO_3 diagram (Fig. 9b), majority of open well and borewell samples falls above and /or nearer to the equiline, which again shows that both silicate and carbonate weathering occurs in the study area. In the post-monsoon season, about 66% of open well samples and 58% of borewell samples have a value greater than 2 and this is due to increase in Ca ions from leaching of Kankar present in the study area. In the bivariate diagram of Ca+Mg *vs* HCO_3+SO_4, majority of the data plots falls on the equiline, both in pre-monsoon and post-monsoon seasons, indicating the role of silicate and carbonate weathering taking place in study area.

In the Ca+Mg *vs* Total cations (TZ) (Fig. 9c), both open well and bore well sample plots fall just below the 1:1 equiline irrespective of the seasons, suggesting the excess input of cations and hence indicate the dominance of chemical weathering (Sami,1992). The plot of Na+K *vs* TZ (Fig. 9d) can be used to decipher the extent of silicate weathering in the study area (Stallard and Edmund, 1983). In the plot of Na+K vs. Total cations, majority of the points fall far away from the 0.5 equiline irrespective of the seasons., which indicates a very low Na^+ and K^+ which is derived from the weathering of silicate rocks in the study area as compared to the Ca^{2+} and Mg^{2+} ions. In the Cl^-+SO_4^{2-} *vs* Na+K scatter diagram (Fig.9f) irrespective of the season majority of samples fall on the 1:1 equiline, which shows that these elements are evolved from the dissolution of rocks present in the study area. But for the post-monsoon certain open well and bore well sampling points fall above the equiline may be due to high Cl^- and SO_4^{2-} concentration. But certain bore well samples, irrespective of the seasons, fall above the equiline which indicates that the excess sulfates are derived from the dissolution of sulfate rich rocks in the study area.

Mineral stability diagram for (a) $CaO–Al_2O_3 –SiO_2 –H_2O$ (b) $MgO–Al_2O_3 –SiO_2 –H_2O$ (c) $Na_2O–Al_2O_3 –SiO_2 –H_2O$ and, (d) $K_2O –Al_2O_3 –SiO_2 –H_2O$ systems were plotted for groundwater samples collected during the pre-monsoon and post-monsoon seasons (Fig. 10). As seen from Fig.10, majority of the samples fall in the stability field of kaolinite. This is indicative of silicate weathering, which will result in the breakdown rock forming minerals into Ca, Mg, Na and K as well as kaolinite which will be left behind in the weathering front. In the $Na_2O–Al_2O_3 –SiO_2 –H_2O$ (Fig. 10c), all the open well and bore well samples in the pre-monsoon and post-monsoon seasons fall in the kaolinite stability field. Na feldspar will dissolve to produce kaolinite and other products when dissolution begins, the water contains

negligible concentrations of $Si(OH)_4$, and Na as the concentrations of these constituent's increase, the water composition, expressed in terms of $Si(OH)_4$ and Na^+/H^+, will plot in the gibbsite stability field. As dissolution continues, $Si(OH)_4$ and the $[Na^+]/[H^+]$ ratio increases, and the water composition moves through the gibbsite stability field into the kaolinite field. Due to the continuous dissolution of the feldspar, the values of $Si(OH)_4$ and $[Na^+]/[H^+]$ increases and the water chemistry evolves toward the Na-feldspar field.

The kaolinite stability field proposes that infiltrating water that is enriched in soil CO_2 reacts with silicate minerals in the host rock, mainly feldspar. The infiltrating water will leach out these alkaline and alkaline earth elements from the weathering front transforming to a more silica-rich clay mineral such as kaolinite.

4.6 Saturation Index

Saturation index (SI) is used as a tool to determine the equilibrium state of water with respect to a mineral phase. The calculation of the SI is useful to identify the minerals in groundwater and to identify the geochemical reactions controlling the water chemistry (Drever,1988). SI of a mineral is defined as the ratio of activity product of ions (IAP) in the solution to the equilibrium solubility product (KT); (Garrels and Mackenise,1967)

The saturation index was calculated based on Equation SI = log (IAP/KT); (Filiz et al., 2000). Majority of the mineral facies are saturated to oversaturated concerning calcite, aragonite, dolomite, and magnesite. The over-saturation of the carbonate minerals may be due to the input excess of Ca^{2+} and Mg^{2+} ions from the various rock types present in the study area. A positive saturation index (SI > 0) reflects that the groundwater is supersaturated with a particular mineral and the tendency of that mineral phase to get precipitated from the groundwater. This indicates that the water is discharged from an aquifer containing a sufficient quantity of mineral and takes a longer residence time to reach equilibrium. SI < 0 signifies undersaturation of a particular mineral which gets dissolved into solution to reach equilibrium concentration (Deutsch, 1997). Groundwater with SI < 0 indicates that groundwater is derived from an aquifer with an insufficient amount of mineral for a solution. The calculated values of SI for calcite, dolomite, aragonite and magnesite in open well samples during the pre-monsoon and post-monsoon seasons (Fig.11) ranges from -2.4 to 0.69, -3.9 to 2.06, -2.5 to -0.53, -3.9 to - 0.267 and -2.41 to 0.67, -3.82 to 1.74, -2.53 to 0.52, -3.24 to -0.48. SI for calcite, dolomite, aragonite, and magnesite in bore well samples during pre-monsoon and post-monsoon ranges from -0.69 to 0.91, 0.88 to 2.55, -0.86 to 0.74, -1.81 to 0.01 and -1.71 to 0.51, -3.46 to 1.90, -1.92 to 0.42, -3.3 to -0.31. The majority of the groundwater samples are saturated to over saturated with respect to calcite, dolomite, and aragonite.

4.7 Corrosion and Scaling

Corrosion and scaling are caused by unique chemistry of groundwater. Water quality components which are important to corrosion and scaling include hardness (as $CaCO_3$), pH, EC (Electrical Conductivity), TDS

(Total Dissolved Solids) and bicarbonate (HCO_3^-), (Rafferty, 2000). Scaling problems usually occur above levels of 100 mg/l hardness and become severe above 200 mg/L. Scaling increases with increasing hardness, calcium concentration, alkalinity, groundwater temperature, and pH. Langelier Saturation Index (LSI) and is a qualitative assessment of water potential to dissolve or precipitate calcium carbonate. LSI is an equilibrium index which deals with the thermodynamic driving force for calcium carbonate scale formation, and it indicates a driving force for scale formation in terms of pH. According to Langelier, the corrosive action of water is mainly due to an excess of free CO_2 and its interaction with carbonates of calcium and magnesium. In the presence of carbon dioxide, these salts are held in solution as bicarbonates, and for any given concentration of calcium and magnesium, there is an equivalent concentration of carbon dioxide to prevent the decomposition of these bicarbonates back into carbonates. LSI values generally lie between −3 and +3. If the LSI value is positive then it indicates that the water is saturated with $CaCO_3$ and the water will deposit $CaCO_3$ as scales which sticks on to boilers, pipes, vessels, and negative index indicates that the water is undersaturated will dissolve $CaCO_3$ and will be considered as corrosive as a result of low alkalinity and high free CO_2 content (Hounslow, 1995; Ravikumar et al.,2011).

The values of the Langelier Saturation Index are illustrated through histograms for both open well (Fig.12a) and bore well samples (Fig.12b) for the pre-monsoon and post-monsoon season. LSI values for open well samples range from -2.2 to 0.97 and -2.4 to 0.4 for pre-monsoon and post-monsoon seasons. Pre-monsoon and post-monsoon LSI values for bore well samples range from -0.65 to 1.07 and -1.68 to 0.89, respectively. From LSI values in the study area, it is observed that about 48% of open well samples (Fig.12a) and 81% of bore well samples (Fig.12b) during pre-monsoon season are supersaturated with positive LSI index and showing tendency to deposit $CaCO_3$. Langelier Index values of all wells decrease during post-monsoon season and this may be due to dilution of groundwater due to precipitation, which causes an increase in CO_2 levels and exhibits corrosion tendency.

The Puckorius Scaling Index (PSI) is used to quantify the amount of precipitation that can form in bringing water to equilibrium. PSI value less than 5 shows that the water intended to be scaling. The result indicated that 46% of pre-monsoon and 35% of post-monsoon open well samples expose scaling tendency (Table 5). PSI index also indicates that the bore well samples have more scaling tendency (viz., 76% pre-monsoon and 57% of post-monsoon) than the open well samples (Fig.12c, 12d).

Among the groundwater samples, the samples collected from the wells OW23, BW20 and BW21 show scale formation while boiling. To understand the physico-chemical characteristics of scale deposit, a few samples are examined under Scanning Electron Microscope (SEM) with Energy Dispersive X-ray Spectroscopy (EDS) facility. The analysis shows that the scales are composed of acicular crystals of $CaCO_3$ (Fig. 13a & 13b). EDS studies of some selected crystals show that, Calcium, Carbon and Oxygen are the major elements present in the scale deposit. Trace of Fe, Mg, Si and Al are also noticed in some crystals. Turner and Smith reported that calcite crystals were observed when the supersaturation ratio (SR) at the temperature of the heat transfer surface was relatively moderate (i.e., 0.90 < LSI < 1.00),

whereas aragonite was observed when the supersaturation was relatively high (i.e., 0.95 < LSI < 1.34). Aragonite, the needle-shaped $CaCO_3$ polymorph, is normally formed at high temperatures, and the composition of the scale is mainly $CaCO_3$.

5.0 Conclusion

The present study focused on the hydrochemical characterization and groundwater of the upper Bhavani river basin of the Attappadi Critical Zone Observatory in Southern Peninsular India. The study was based on the 88-groundwater samples, from both open well and bore wells, collected during the pre-monsoon and post-monsoon seasons. It was observed that the major cations and anions in the groundwater samples for both seasons are in the order: Ca^{2+}> Mg^{2+} >Na^{+} >K^{+} and HCO_3^{-}>Cl^{-}>SO_4^{2-}. Except for a few, the majority of the chemical parameters are well within the permissible limit set by WHO, and ionic concentrations are generally high for the pre-monsoon season than the post-monsoon season. This may be due to the input of rainwater during the post-monsoon season. The application of PCA and HCA on the available data indicated that the water quality variations are mainly due to geogenic/natural processes. However anthropogenic factors also had significant effect in the agricultural/settlement dominated areas. It was observed that about 52% of water samples are supersaturated with carbonate minerals (calcite, dolomite, and aragonite). Saturation Index and mineral stability diagram also support that the incongruent dissolution of aluminosilicate minerals (silicate weathering), which is an important hydrochemical process controlling the chemistry of groundwater. LSI and PSI indices show that majority open well and bore well samples show scaling tendency. It was observed that, among the contributing factors that determine the hydrochemical characteristics of well water samples, both silicate and carbonate weathering and agricultural activities plays a pivotal role in the input of ions to the groundwater in the area. Long-term monitoring of the hydrochemical characteristics of the groundwater in the region will unravel the source contribution and future trends of hydrochemical characteristics of the groundwater systems in intensely managed agricultural systems in arid and semi-arid regions.

Declarations

Acknowledgements

We thank the Director, National Centre for Earth Science Studies (NCESS) for facilities, encouragement and support. First author is thankful to the Kerala Science Technology and Environment (KSCSTE), Fellowship No.001/FSHP/-MAIN/2015/KSCSTE for financial support. VTR acknowledges DST, New Delhi for financial assistance through INSPIRE Fellowship (No: DST/INSPIRE Fellowship/[IF160550]). We are thankful to Dr. Arulbalaji P for assisting and guiding for the field works and sample collection.

Funding: GJA - Research was supported by Kerala Science Technology and Environment (KSCSTE), Fellowship No.001/FSHP/-MAIN/2015/KSCSTE for financial support.

VTR - Research was supported by DST, New Delhi for financial assistance through INSPIRE Fellowship (No: DST/INSPIRE Fellowship/[IF160550]).

Conflicts of interest/Competing interests: The authors declare that they have no known competing financial interests or personal relationships that could have appeared to influence the work reported in this paper.

Availability of data and material: Data included as electronic supplementary material

Code availability: Not Applicable

Authors' contributions: GJA, VTR, KS, PD: Conceptualization, Methodology and Analysis. GJA, VM and KS: Statistical Analysis and Visualization KS, KM and PD: Supervision, Writing- Reviewing and Editing.

References

André, L., Franceschi, M., Pouchan, P., & Atteia, O. (2005). Using geochemical data and modelling to enhance the understanding of groundwater flow in a regional deep aquifer, Aquitaine Basin, south-west of France. *Journal of Hydrology*, *305*(1-4), 40-62.

Back, W. (1966). Hydrochemical facies and ground water flow patterns in northern part of Atlantic Coastal Plain. USGS Professional Paper 498-A.

Barzegar, R., Moghaddam, A. A., & Tziritis, E. (2017). Hydrogeochemical features of groundwater resources in Tabriz plain, northwest of Iran. *Applied Water Science*, *7*(7), 3997-4011.

Chandran, S., Karmegam, M., Kumar, V., & Dhanasekarapandian, M. (2017). Evaluation of groundwater quality in an untreated wastewater irrigated region and mapping—a case study of Avaniyapuram sewage farm, Madurai. *Arabian Journal of Geosciences*, *10*(7), 159.

Closs, L. G., & Nichol, I. (1975). The role of factor and regression analysis in the interpretation of geochemical reconnaissance data. *Canadian Journal of Earth Sciences*, *12*(8), 1316-1330.

Deutsch, W. J. (1997) Groundwater geochemistry: fundamentals and applications to contamination, CRC press, Boca Raton, Florida.510p.

Drever, J. I. (1988). The Geochemistry of Natural Waters Prentice-HalL Inc. *Englewood Cliffe, NJ*.

Edmunds, W. M., Carrillo-Rivera, J. J., & Cardona, A. (2002). Geochemical evolution of groundwater beneath Mexico City. *Journal of Hydrology*, *258*(1-4), 1-24.

Ekwere, A. S., & Edet, A. (2012). Hydrogeochemical signatures of different aquifer layers in the crystalline basement of Oban area (SE Nigeria). *Journal of Geography and Geology*, *4*(1), 90.

Elgallal, M., Fletcher, L., & Evans, B. (2016). Assessment of potential risks associated with chemicals in wastewater used for irrigation in arid and semiarid zones: A review. *Agricultural Water Management*, *177*, 419-431.

Federation, W. E., & American Public Health Association. (1995). Standard methods for the examination of water and wastewater. *American Public Health Association (APHA): Washington, DC, USA*.

Federation, W. E., & American Public Health Association. (2005). Standard methods for the examination of water and wastewater. *American Public Health Association (APHA): Washington, DC, USA*.

Filiz, S., Tarcan, G., & Gemici, U. (2000, May). Geochemistry of the Germencik geothermal fields, Turkey. In Proceedings of the World Geothermal Congress (pp. 1115-1120).

Garrels, R. M., & mackenzie, F. T. (1967). Origin of the chemical compositions of some springs and lakes.

Gerla P.J., (1992). The relationship of water-table changes to the capillary fringe, evapotranspiration. and pre- cipitation in intermittent wedands. Wetlands, 12(2): 91-98.

Guo, H., & Wang, Y. (2005). Geochemical characteristics of shallow groundwater in Datong basin, northwestern China. Journal of Geochemical Exploration, 87(3), 109-120.

Hallouche, B., Marok, A., Benaabidate, L., Berrahal, Y., & Hadji, F. (2017). Geochemical and qualitative assessment of groundwater of the High Mekerra watershed, NW Algeria. Environmental Earth Sciences, 76(9), 340.

Hosseinifard, S. J., & Aminiyan, M. M. (2015). Hydrochemical characterization of groundwater quality for drinking and agricultural purposes: a case study in Rafsanjan plain, Iran. *Water Quality, Exposure and Health*, *7*(4), 531-544.

Hounslow, A.W. (1995). Water Quality Data Analysis and Interpretation, New York, NY, USA: Lewis Publishers.

Jampani, M., Huelsmann, S., Liedl, R., Sonkamble, S., Ahmed, S., & Amerasinghe, P. (2018). Spatio-temporal distribution and chemical characterization of groundwater quality of a wastewater irrigated system: a case study. *Science of the Total Environment*, *636*, 1089-1098.

Jeong, C. H. (2001). Effect of land use and urbanization on hydrochemistry and contamination of groundwater from Taejon area, Korea. *Journal of Hydrology*, *253*(1-4), 194-210.

Kaushal, S.S., Duan, S., Doody, T.R., Haq, S., Smith, R.M., Johnson, T.A.N., Newcomb, K.D., Gorman, J., Bowman, N., Mayer, P.M. and Wood, K.L. (2017). Human-accelerated weathering increases salinization, major ions, and alkalinization in fresh water across land use. *Applied Geochemistry*, *83*, pp.121-135.

Kolsi, S. H., Bouri, S., Hachicha, W., & Dhia, H. B. (2013). Implementation and evaluation of multivariate analysis for groundwater hydrochemistry assessment in arid environments: a case study of Hajeb Elyoun–Jelma, Central Tunisia. *Environmental earth sciences*, *70*(5), 2215-2224.

Langelier, W. F. (1936). The analytical control of anti-corrosion water treatment. Journal-American Water Works Association, 28(10), 1500-1521

Loh, Y. S. A., Yidana, S. M., Banoeng-Yakubo, B., Sakyi, P. A., Addai, M. O., & Asiedu, D. K. (2016). Determination of the mineral stability field of evolving groundwater in the Lake Bosumtwi impact crater and surrounding areas. *Journal of African Earth Sciences*, *121*, 286-300.

Mayo, A. L., & Loucks, M. D. (1995). Solute and isotopic geochemistry and ground water flow in the central Wasatch Range, Utah. *Journal of Hydrology*, *172*(1-4), 31-59.

Meybeck, M., Green, P., & Vörösmarty, C. (2001). A new typology for mountains and other relief classes. *Mountain Research and Development*, *21*(1), 34-45.

Mining and Geology (2016). District Survey Report of Minor Minerals, Palakkad District.

Morán-Ramírez, J., Ledesma-Ruiz, R., Mahlknecht, J., & Ramos-Leal, J. A. (2016). Rock–water interactions and pollution processes in the volcanic aquifer system of Guadalajara, Mexico, using inverse geochemical modeling. Applied Geochemistry, 68, 79-94.

Nair, R. V. G., Nair, M. M., & Maji, A. K. (2005). Gold mineralization in Kottathara prospect, Attappadi Valley, Kerala, India: a preliminary appraisal. *Gondwana Research*, *8*(2), 203-212.

Nambiar, A.R. (1982). Report on the geological mapping and geochemical exploration for precious metals in parts of Attapadi area, Palghat district, Kerala. Unpub. Prog. Rep., Geol. Surv. India

Padmalal D., Remya S.I., Jissy Jyothi S., Baijulal B., Babu K.N. and Baiju R.S. (2011). Water quality and dissolved inorganic fluxes of N, P, SO4, and K of a small catchment river in the Southwestern Coast of India. Environment Monitoring and Assessment. Vol.184, No.3, pp. 1541-1567.

Peisert, C., & Sternfeld, E. (2005). Quenching Beijing's thirst: the need for integrated management for the endangered Miyun reservoir. *China Environment Series*, *7*, 33-45.

Pincetti-Zúniga, G.P., Richards, L.A., Tun, Y.M., Aung, H.P., Swar, A.K., Reh, U.P., Khaing, T., Hlaing, M.M., Myint, T.A., Nwe, M.L. and Polya, D.A. (2020). Major and trace (including arsenic) groundwater chemistry in central and southern Myanmar. *Applied Geochemistry*, *115*, p.104535.

Piper, A. M. (1953). *A graphic procedure for the geo-chemical interpretation of water analysis. USGS groundwater* (No. 12). note.

Rafferty, K.D., (2000). Scaling in geothermal heat pump systems. GHC Bulletin, 21, 11–15.

Rao, N. S., Sunitha, B., Sun, L., Spandana, B. D., & Chaudhary, M. (2019). Mechanisms controlling groundwater chemistry and assessment of potential health risk: a case study from South India. Geochemistry, 125568.

Ravikumar, P., Somashekar, R. K., & Angami, M. (2011). Hydrochemistry and evaluation of groundwater suitability for irrigation and drinking purposes in the Markandeya River basin, Belgaum District, Karnataka State, India. *Environmental monitoring and assessment*, *173*(1-4), 459-487.

Sadoff, C., & Muller, M. (2009). *Water management, water security and climate change adaptation: early impacts and essential responses*. Stockholm: Global Water Partnership.

Sami, K. (1992). Recharge mechanisms and geochemical processes in a semi-arid sedimentary basin, Eastern Cape, South Africa. *Journal of Hydrology*, *139*(1-4), 27-48.

Santosh, M., Shaji, E., Tsunogae, T., Mohan, M. R., Satyanarayanan, M., & Horie, K. (2013). Suprasubduction zone ophiolite from Agali hill: petrology, zircon SHRIMP U–Pb geochronology, geochemistry and implications for Neoarchean plate tectonics in southern India. Precambrian Research, 231, 301-324.

Selle, B., Schwientek, M., & Lischeid, G. (2013). Understanding processes governing water quality in catchments using principal component scores. *Journal of Hydrology*, *486*, 31-38.

Sivakarun, N., Udayaganesan, P., Chidambaram, S., Venkatramanan, S., Prasanna, M. V., Pradeep, K., & Panda, B. (2020). Factors determining the hydrogeochemical processes occurring in shallow groundwater of coastal alluvial aquifer, India. Geochemistry, 80(4), 125623.

Sophocleous, M. (2010) Review: groundwater management practices, challenges, and innovations in the High Plains aquifer, USA-lessons and recommended actions Hydrogeol. J. 18, 559–75.

Stallard, R. F., & Edmond, J. M. (1983). Geochemistry of the Amazon: 2. The influence of geology and weathering environment on the dissolved load. *Journal of Geophysical Research: Oceans*, *88*(C14), 9671-9688.

Tyagi, S., & Sarma, K. (2020). Qualitative assessment, geochemical characterization and corrosion-scaling potential of groundwater resources in Ghaziabad district of Uttar Pradesh, India. Groundwater for Sustainable Development, 10, 100370.

Vaux H Jr (2007) The economics of groundwater resources and the American experience. The global importance of groundwater in the 21st century. In: Proceedings of the international symposium on groundwater sustainability, Alicante, Spain. National Ground Water Association Press, Westerville, pp 167–176

Vaux, H. (2011). Groundwater under stress: the importance of management. Environmental Earth Sciences, 62(1), 19-23.

Voutsis, N., Kelepertzis, E., Tziritis, E., & Kelepertsis, A. (2015). Assessing the hydrogeochemistry of groundwaters in ophiolite areas of Euboea Island, Greece, using multivariate statistical methods. *Journal of Geochemical Exploration*, *159*, 79-92.

Wu, J., Wang, L., Wang, S., Tian, R., Xue, C., Feng, W., & Li, Y. (2017). Spatiotemporal variation of groundwater quality in an arid area experiencing long-term paper wastewater irrigation, northwest China. *Environmental Earth Sciences*, *76*(13), 460.

Zhu, Y., Wu, Y., & Drake, S. (2004). A survey: obstacles and strategies for the development of ground-water resources in arid inland river basins of Western China. *Journal of Arid Environments*, *59*(2), 351-367.

Tables

Table 1: Summary statistics for the chemical analysis of open well samples during Pre-monsoon

and Post-monsoon seasons

	Pre-monsoon Open well (PRM)				Post-monsoon Open well (POM)					
Parameters	Min.	Max.	Avg.	Std. dev	Min.	Max.	Avg.	Std. dev	WHO* (2017)	BIS* (2012)
pH	6.1	7.87	7.10	0.44	6.1	7.57	6.83	0.41	8.5	6.5-8.5
EC	154	1260	705	308	77	1046	540	288	500	500
TDS	100	830	469	210	50	680	440	261	500	500
TH	51	854	298	177	50	680	351	187	200	200
Ca^{2+}	7.22	92.2	52.3	26	4.008	120	56	33	100	75
Mg^{2+}	6.2	56.7	23	14	2.47	31	12	7	50	30-100
Na^{+}	3.8	45.7	25.8	11	1.6	35.1	12.64	11.15	200	-
K^{+}	1.1	12.6	3.9	3	0.37	10.3	3.3	2.3	20	-
HCO_3^{-}	50	540	268	139	25	420	194	121	200	600
Cl^{-}	7.1	74	39	12	5.32	52	30	16.3	250	250-1000
SO_4^{2-}	3.66	50.7	21	14	2.16	35	15	10	250	200-400

Table 2: Summary statistics for the chemical analysis of bore well samples during Pre-monsoon and Post-monsoon season

	Pre-monsoon				Post-monsoon					
Parameters	Min.	Max.	Avg.	Std. dev	Min.	Max.	Avg.	Std. dev	WHO* (2017)	BIS* (2012)
pH	6.7	7.94	7.43	0.30	6.5	7.9	7.1	0.33	8.5	6.5-8.5
EC	330	2338	1132	474	246	1575	824	400	500	500
TDS	230	1515	750	306	138	1037	539	262	500	500
TH	98	774	381	163	24.18	631	251	160	200	200
Ca^{2+}	22	185	88	38	28	168.33	91	42	100	75
Mg^{2+}	10	78	38	19	2.35	58.56	23	17	50	30-100
Na^{+}	12	84	41	22	1.6	60.1	23.3	17.4	200	-
K^{+}	2.6	14.4	6	3	1.1	9.2	4.7	2.03	20	-
HCO_3^{-}	100	660	400	143	54	580	298	142	200	600
Cl^{-}	14	102	44	27	10	96.5	39	24	250	250-1000

All values are in mg/l except pH, EC (US/cm^{-1}) *Permissible limit

Table 3: Results of the Principal Component Analysis of Open well and Bore well

	Open Well				Borewell					
	Post-monsoon		Pre-monsoon		Post-monsoon			Pre-monsoon		
Eigen Value	5.49	1.29	6.13	1.27	4.88	1.35	1.12	4.97	1.60	1.16
Explained Variance (%)	60.99	14.38	68.12	14.10	54.27	14.96	12.45	55.21	17.73	12.84
Cumulative (%)	60.99	75.34	68.12	82.22	54.27	69.24	81.68	55.21	72.94	85.77
Variable	*PC1*	*PC2*	*PC1*	*PC2*	*PC1*	*PC2*	*PC3*	*PC1*	*PC2*	*PC3*
TDS	**0.97**	0.24	**0.94**	0.31	**0.85**	0.52	0.08	**0.97**	0.18	0.07
Ca	**0.94**	0.20	**0.92**	0.30	**0.82**	0.39	0.17	**0.90**	0.09	0.17
Mg	**0.81**	0.24	**0.87**	0.31	**0.88**	0.29	-0.08	**0.89**	0.37	-0.04
Na	**0.66**	-0.04	**0.80**	0.08	0.35	**0.81**	-0.23	**0.86**	-0.02	0.11
K	0.20	**0.91**	0.17	**0.88**	0.08	**0.76**	0.08	0.17	**0.84**	-0.33
HCO3	**0.95**	0.26	**0.92**	0.32	0.61	0.60	0.18	**0.82**	0.28	0.16
Cl	**0.58**	-0.04	**0.83**	0.09	0.22	**0.79**	-0.01	0.09	**0.85**	0.25
SO4	**0.67**	**0.62**	**0.57**	**0.65**	0.87	-0.20	-0.17	**0.85**	-0.27	-0.13
SiO4	**0.73**	-0.42	**0.78**	-0.40	0.00	-0.04	**0.98**	0.10	-0.03	**0.97**

Table 4: Correlation analysis between the Principal Component scores and climatic and topographic variables.

Variables	Open Well		Borewell		
	PC1	PC2	PC1	PC2	PC3
Rainfall	**-0.74**	-0.12	-0.35	0.12	-0.19
Potential Evapotranspiration (PET)	-0.06	0.13	-0.22	-0.16	-0.26
Evapotranspiration (ET)	**-0.76**	-0.05	**-0.51**	0.04	-0.39
PET/Rainfall	**0.62**	0.17	0.20	-0.21	0.03
Elevation	-0.25	0.11	-0.41	-0.41	-0.38
Slope	-0.23	0.10	-0.22	**-0.44**	-0.29

Table 5: LSI and PSI values of groundwater water samples in Upper Bhavani basin

Parameters	Index value	Appearance	Number of samples (in %)			
			Pre-monsoon open well (n=23)	Post-monsoon open well (n=21)	Pre-monsoon bore well (n=23)	Post-monsoon bore well (n=21)
Langelier Saturation Index(LSI)	<0	Water is under-saturated with respect to $CaCO_3$,No potential to scale formation	52	82.6	19	38
	>0	Water is supersaturated with respect to CaCO3 and scale forming may occur	48	17.4	81	62
	0	Water is with CaCO3 and scale formation can occur.	-	-		-
Puckorius Scaling Index	<5.5	Heavy scaling	13	13	52	43
	5.5-6.2	Scaling	33	22	24	14
	6.2-6.8	No scale	47	13	19	19
	6.8-8.5	Aggressive	7	22	5	19
	>8.5	Very aggressive	-	30	-	1

Figures

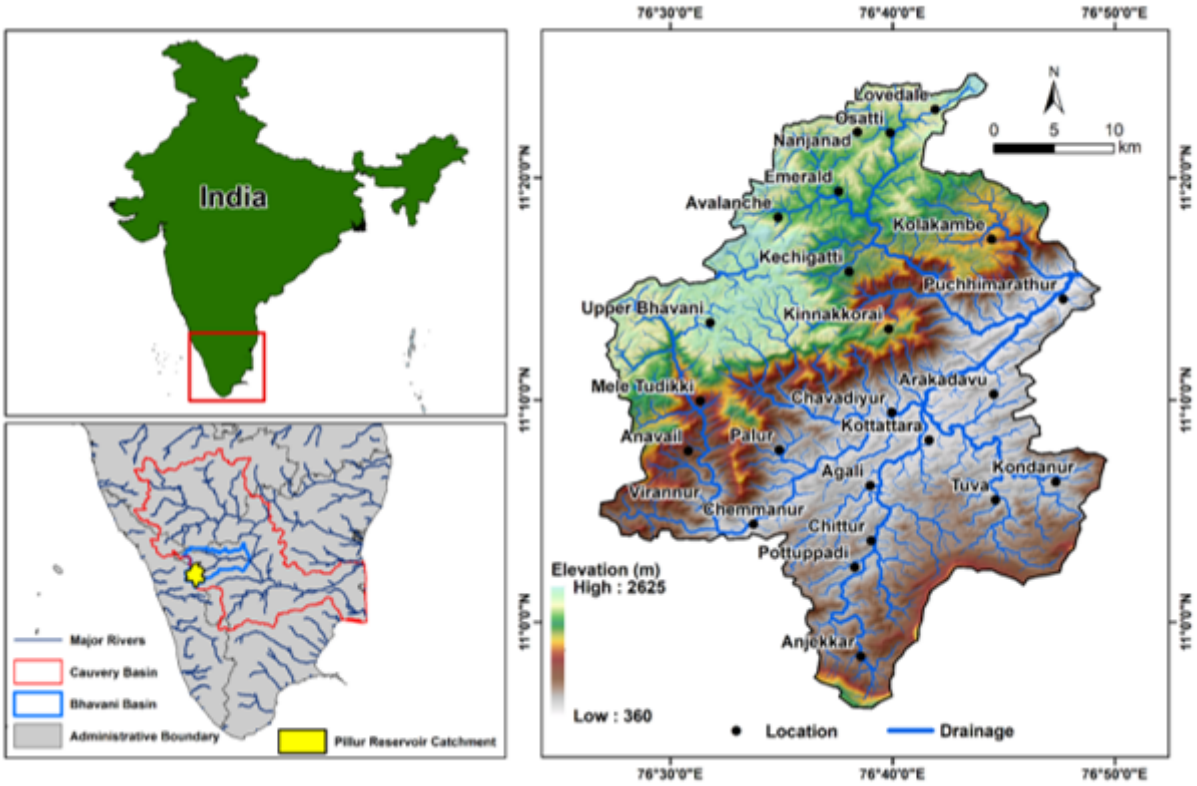

Figure 1

Location of the study area and terrain elevation model. Note the plateau in the north eastern part of the watershed.

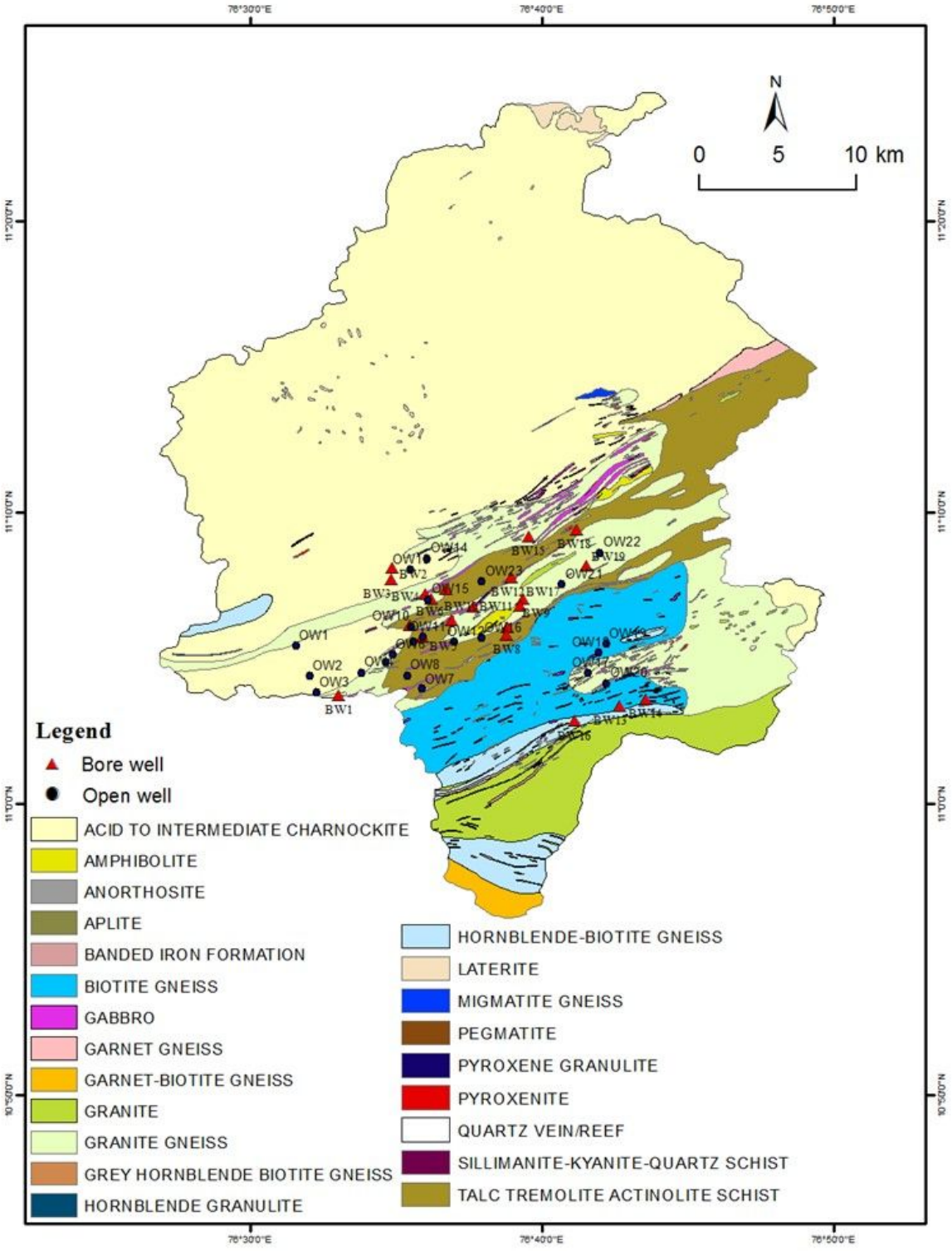

Figure 2

Geology map of the study area showing the locations of open and bore wells sampled in the present study

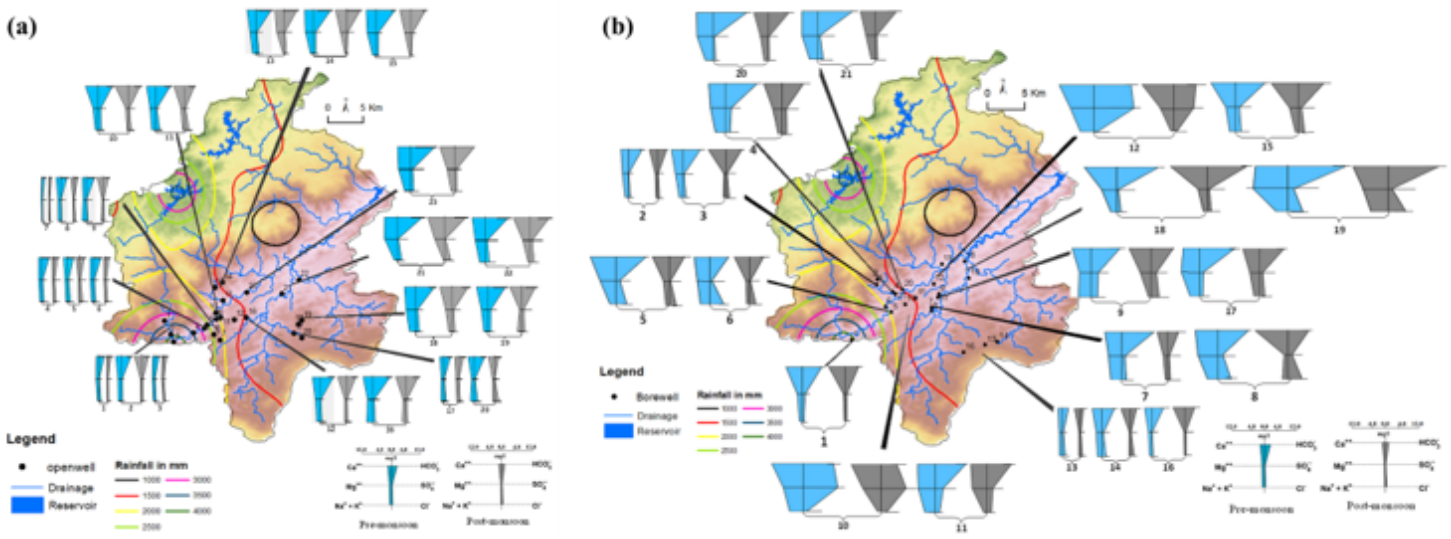

Figure 3

Spatial variation of cations and anions in pre-monsson and post-monsoon season in the (a) open wells and (b) bore wells samples

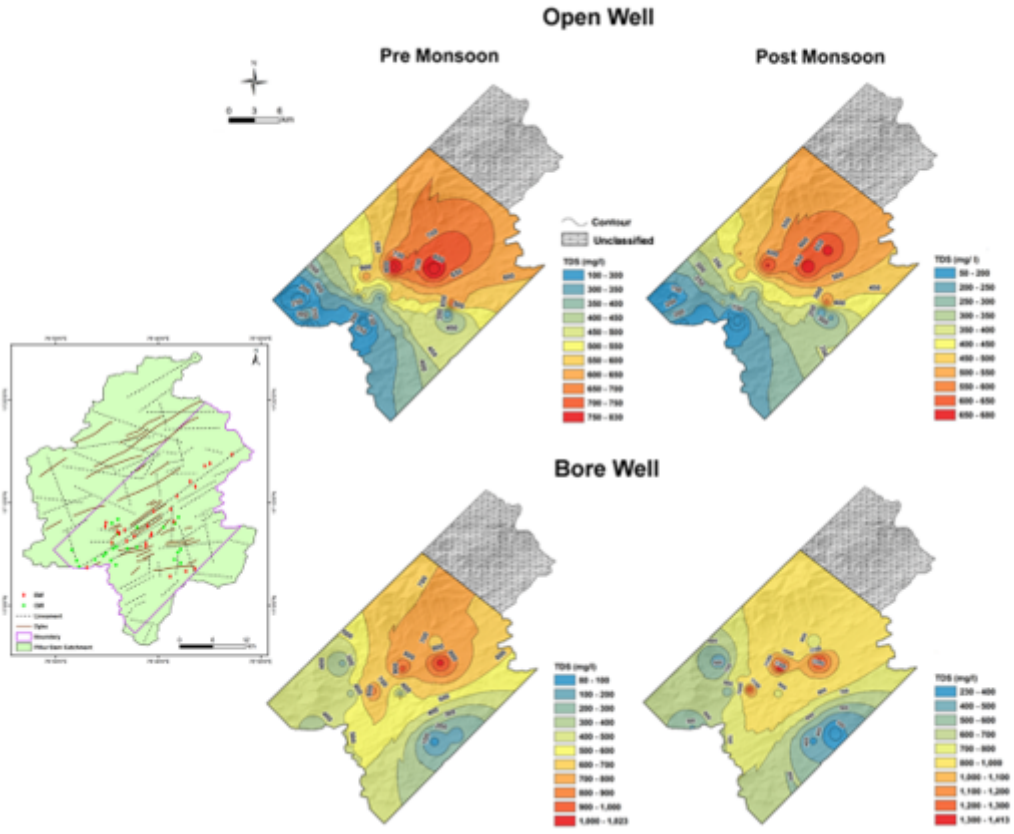

Figure 4

Spatial variation map of total dissolved solids for open well, bore well samples during pre- monsoon, and post - monsoon season

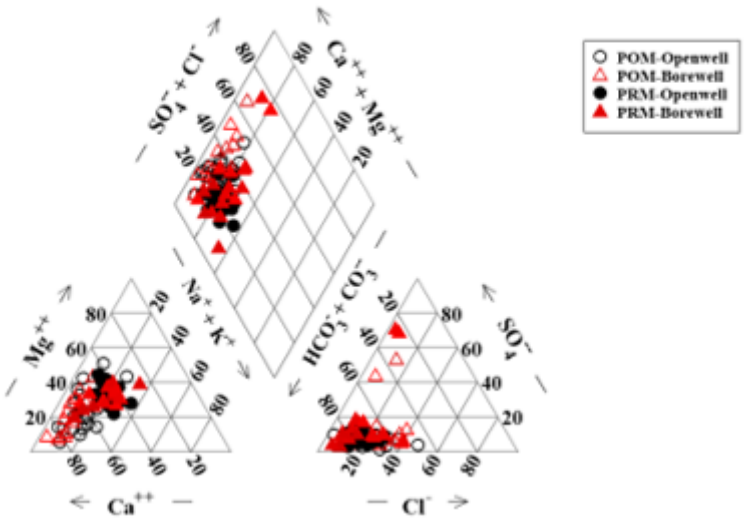

Figure 5

Piper diagram of the groundwater samples in the study area

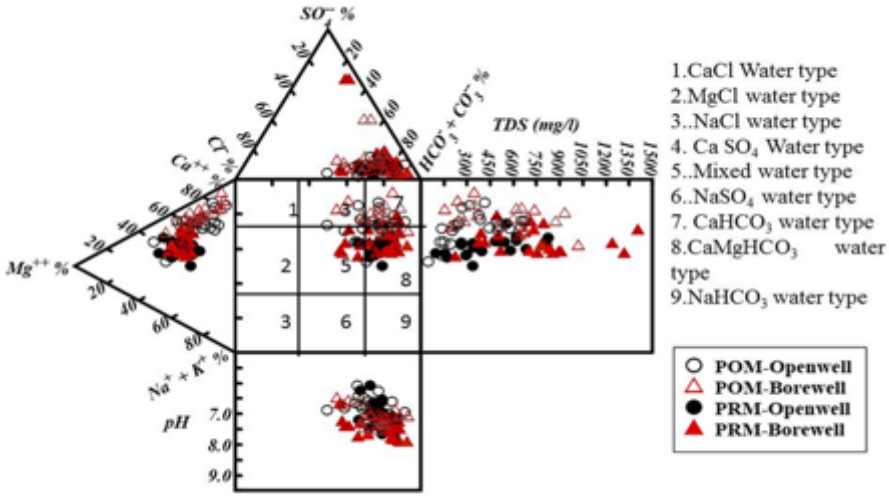

Figure 6

Durov diagram of the groundwater samples in the study area

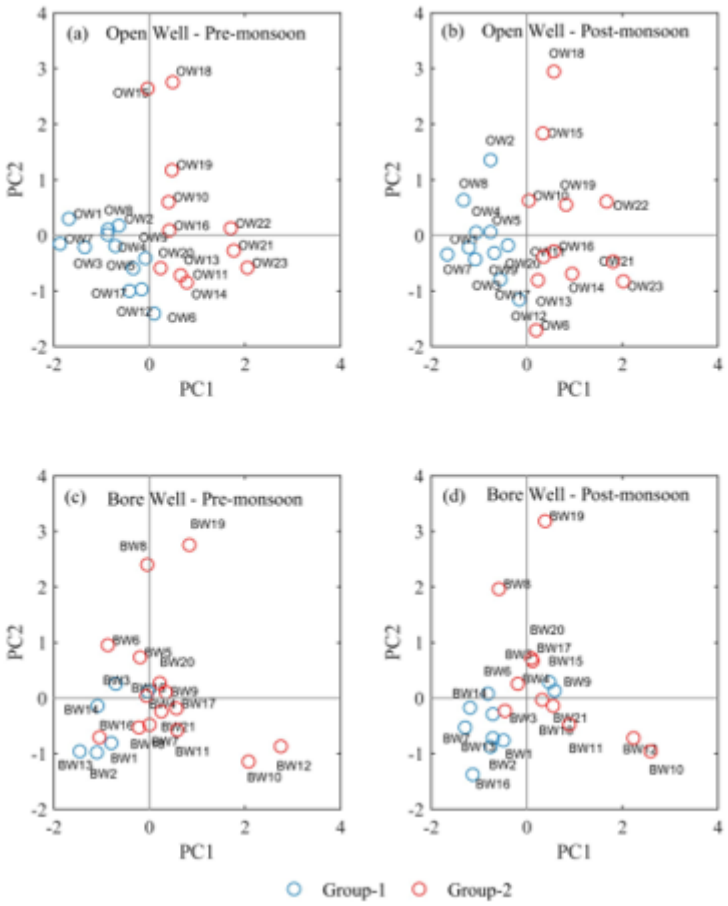

Figure 7

Scatter plot showing the spatial patterns of the principal component loadings for (a) Pre-monsoon samples and (b) Post-monsoon samples in Open wells; and (c) Pre-monsoon samples and (d) Post-monsoon samples in Bore wells

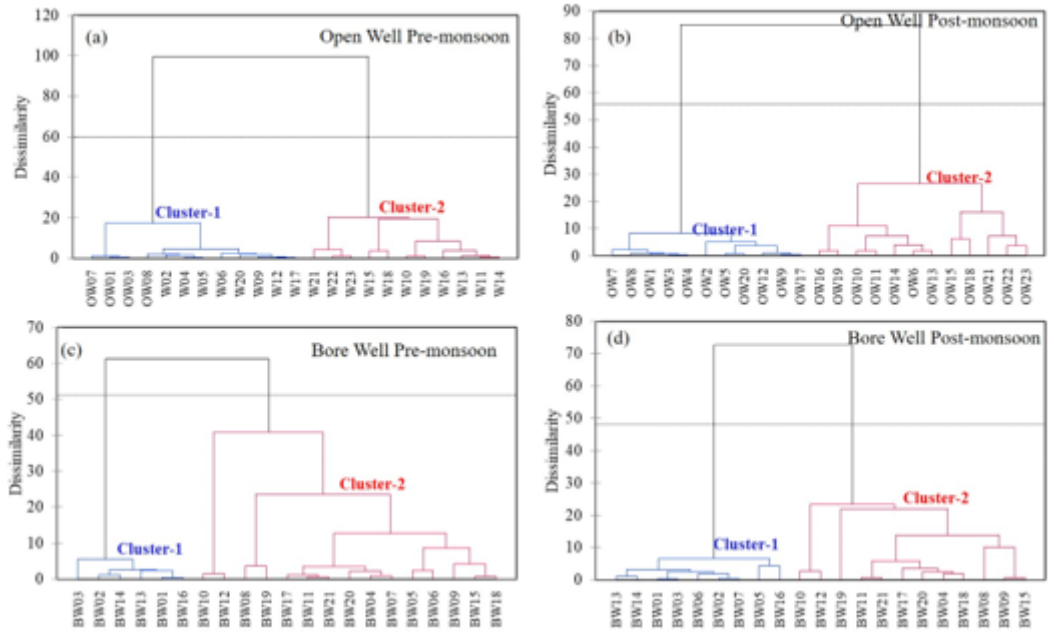

Figure 8

Dendrogram of the Agglomerative Hierarchical Clustering (AHC) analysis using the Ward method for (a) Pre-monsoon (b) Post-monsoon samples of open well and (c) Pre-monsoon (d) Post-monsoon samples of Bore well samples.

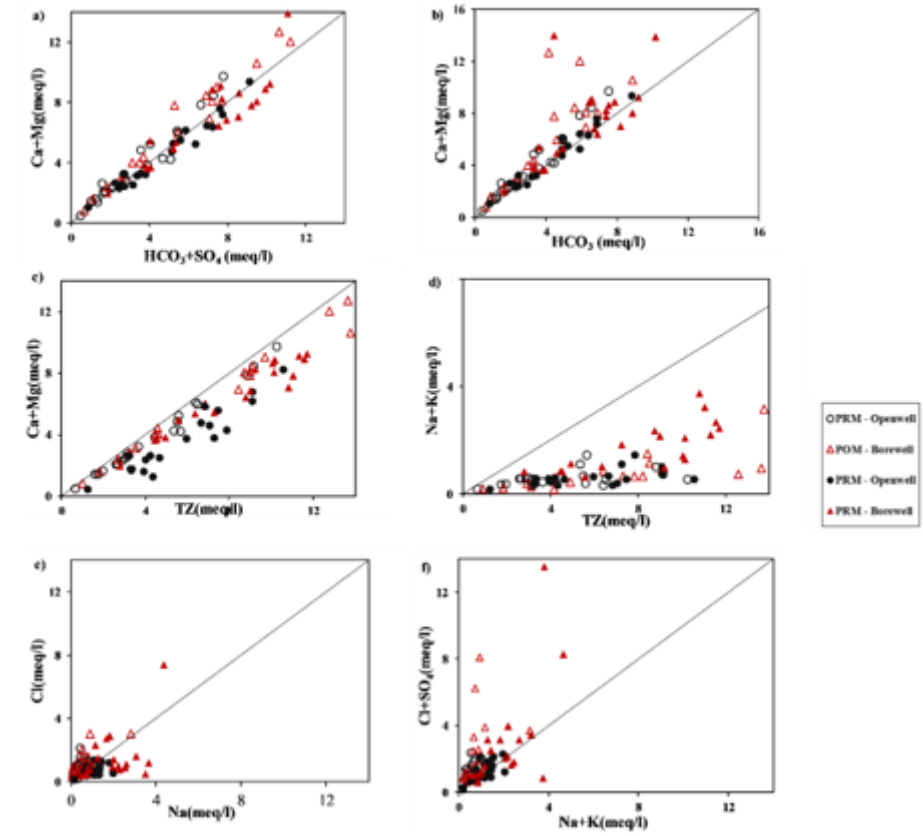

Figure 9

Scatter plots for (a) Ca+Mg vs HCO3+SO4, (b) Ca+Mg vs HCO3+SO4, (c) Ca+Mg vs TZ, (d)Na+K vs TZ, (e)Na vs Cl and(f) Na+ vs Cl+ SO4

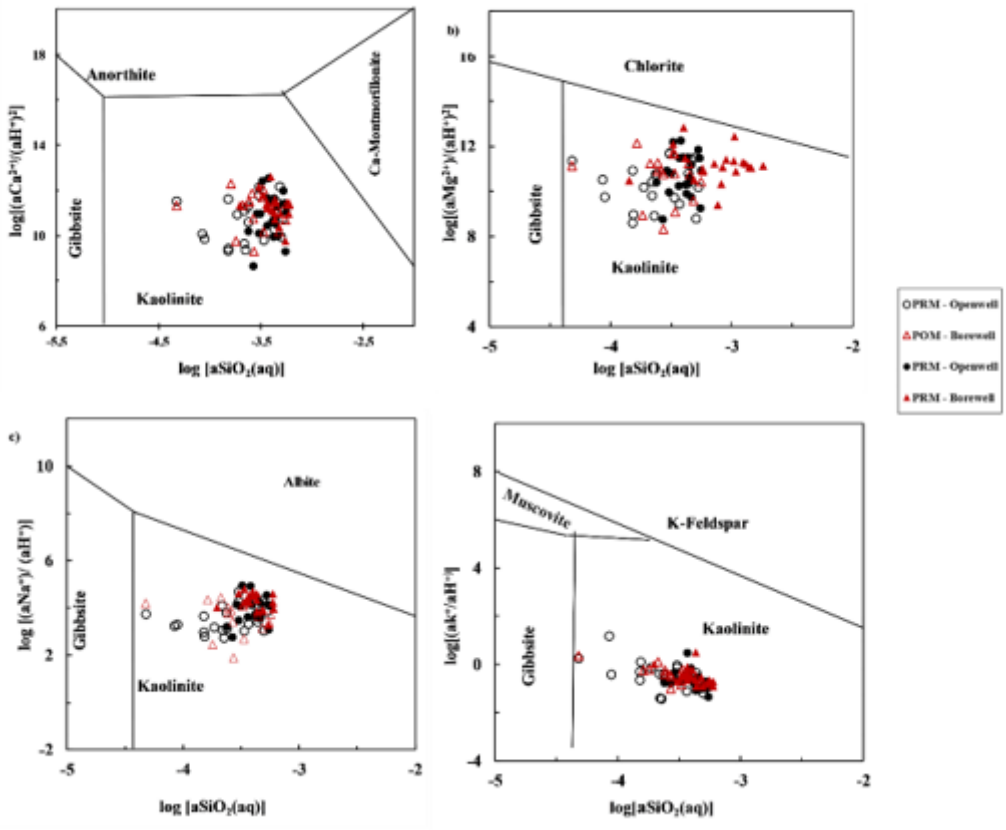

Figure 10

Mineral stability diagrams of (a) CaO–Al2O3 –SiO2 –H2O (b) MgO–Al2O3 –SiO2 –H2O (c) Na2O–Al2O3 –SiO2 –H2O and (d) K2O –Al2O3 –SiO2 –H2O system

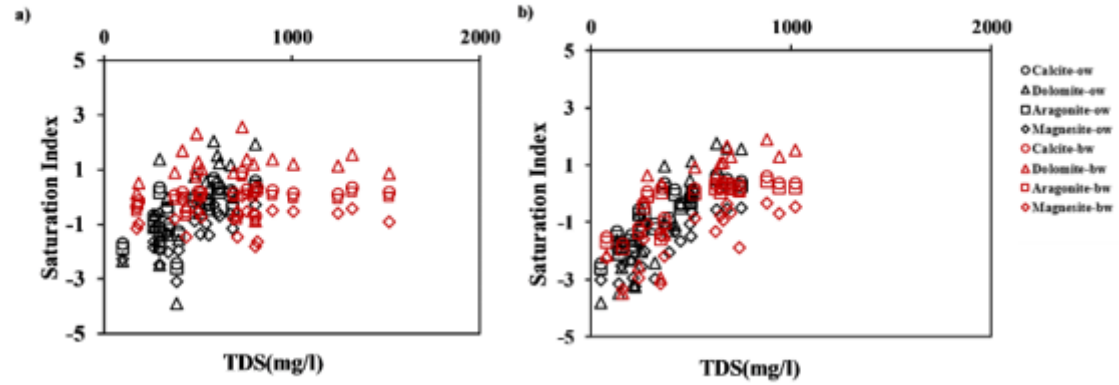

Figure 11

Plots of Saturation Indexes with respect to TDS for (a) Pre-monsoon and (b) Post-monsoon (*ow=Openwell,*bw=Borewell)

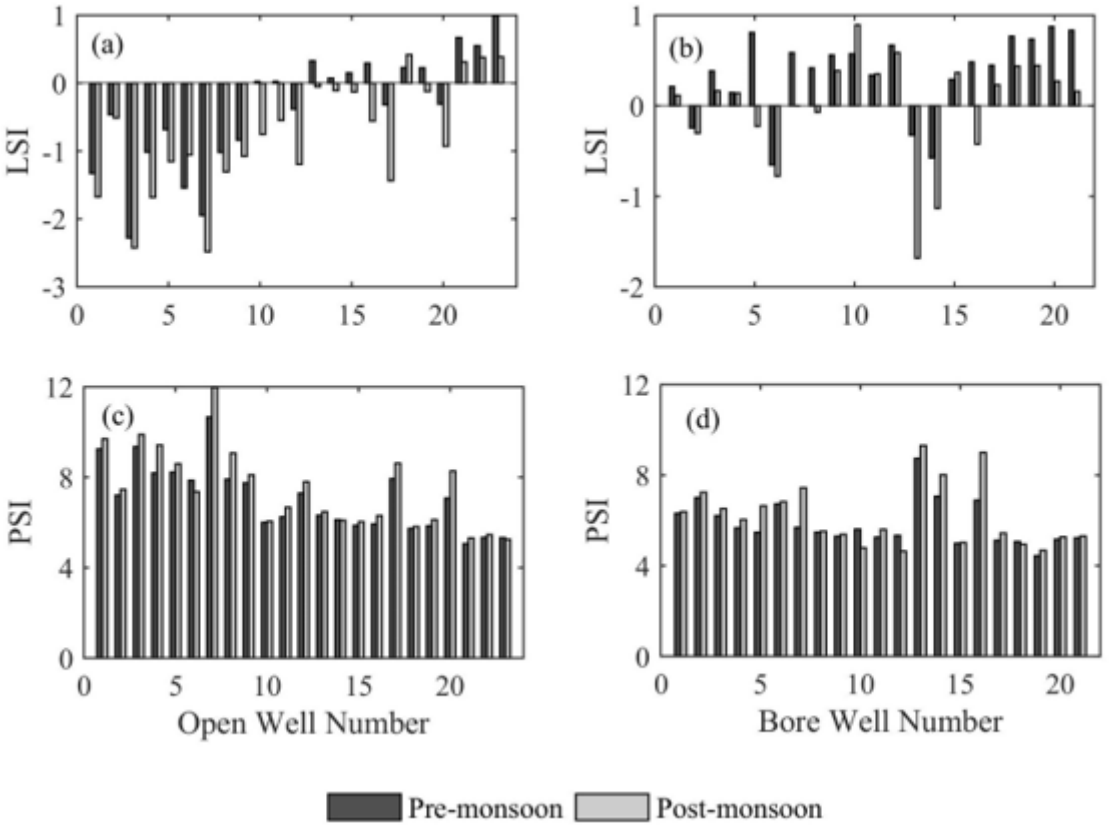

Figure 12

Seasonal evaluation of (i) LSI for (a) Open well and (b) Bore well and (ii) PSI values for (c) Open well and (d) Bore well samples

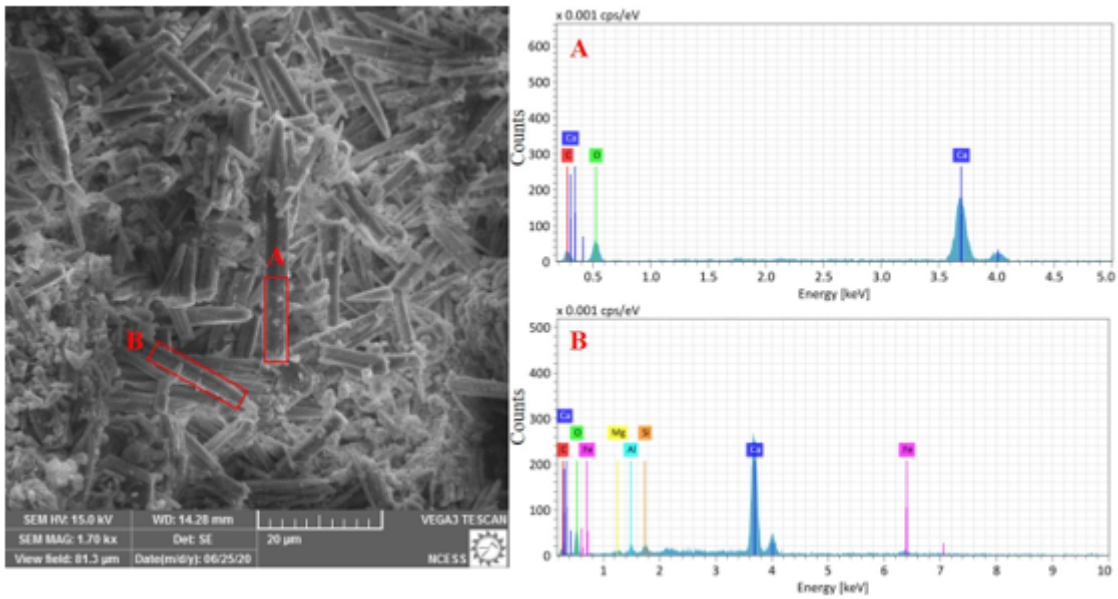

Figure 13

Scanning electron micrograph (a) and energy dispersive spectrum (b) for natural scale deposit sample.

Supplementary Files

This is a list of supplementary files associated with this preprint. Click to download.

- Supplementarymaterial.pdf